High-Q Resonator with Integrated Capacitance for Resonance Power Conversion

Phyo Aung Kyaw
Aaron L. F. Stein
Charles R. Sullivan

In IEEE Applied Power Electronics Conference (APEC), pp. 2519-2526, March 2017

High-Q Resonator with Integrated Capacitance for Resonant Power Conversion

Phyo Aung Kyaw, Aaron L.F. Stein, Charles R. Sullivan
Thayer School of Engineering at Dartmouth
Hanover, NH 03755, USA
{phyo.a.kyaw.th, aaron.l.stein, charles.r.sullivan}@dartmouth.edu

***Abstract*—Resonant power conversion at MHz frequencies is useful for miniaturization of power electronics, but requires resonators or inductors with high efficiency. Because litz wire is not effective above several MHz, an alternative winding structure for inductors is required for operation at these frequencies. In this paper, we present resonators with a multi-layer foil winding which can be constructed using industry-standard polyimide laminates. The proximity effect losses are reduced due to current sharing between multiple conductor layers much thinner than a skin depth. The integrated capacitance of the resonator eliminates the need for a physical connection between the inductor and the capacitor required in a typical LC resonant tank. Low-loss NiZn ferrite cores were used to straighten field lines to reduce lateral current crowding. Prototypes of both parallel and series resonators achieved quality factors over 800 in the 7–9 MHz range, confirming the theoretical analysis of multi-layer foil windings.**

I. Introduction

Passive components, especially magnetics, dominate the size and loss of switching power converters and are increasingly the main bottleneck in miniaturization of power electronics. High-frequency operation reduces the energy storage and ripple requirements, and thus, is useful for miniaturization. However, frequency dependent switching and conduction losses must be minimized to realize these benefits. Zero-voltage switching (ZVS) and resonant gating can be used to reduce the frequency dependent switching losses associated with charging and discharging capacitances and device gates [1]–[3]. Advances in wide-bandgap semiconductors such as GaN and SiC allows for high power levels at high switching frequencies and there is renewed interest in increasing the switching frequency to the MHz range and beyond [1], [4]–[6]. However, high frequency conduction losses in magnetics, especially due to the proximity effect, need to be addressed to realize the benefits of high switching frequency and wide-bandgap devices in power conversion.

Capacitors in general have higher energy density and lower losses than inductors and some power conversion architectures such as switched-capacitor (SC) converters solely use switches and capacitors [7] to avoid inductor losses. Even in these SC converters, adding a small inductance to form resonant switched-capacitor circuits facilitates soft switching and variable conversion ratios [8]–[10]. In other power conversion architectures, such as series resonant converters, which use LC resonant tanks, soft switching also helps reduce frequency dependent switching losses.

Thus, a high-Q resonator, or a low-loss inductor for resonance, for the MHz frequency range is desirable. Resonators with lower losses, compared to conventional LC tanks using litz-wire inductors, can be used in resonant power converters to achieve better efficiency, or a smaller size for the same power rating and allowable temperature rise. A series resonator with a high quality factor may simply replace discrete LC tanks in series resonant converters. Parallel resonators are less common in power electronics, but broader adoption of converter topologies based on parallel resonators, such as those in [11]–[14], could be motivated if relatively easy to construct very high-Q parallel resonators are available.

Up to around 1 MHz, proximity effect losses in inductors can be effectively handled using litz wire. Above 1 MHz, however, litz wire becomes increasingly cost prohibitive since the required wire strands for effective loss reduction become extremely fine and are not commercially available. However, free standing metal foils of 16 μm thickness are found in grocery stores and foils as thin as 5 μm are available [15]. In litz wire, twisting the wire strands forces equal current sharing among strands; however, metal foils cannot be twisted in a similar manner, and strategies such as layer interchange and capacitive ballasting [15] are necessary to achieve equal current sharing among different layers.

A multi-layer foil winding with capacitive ballasting is used in [16] for a parallel self-resonant structure for wireless-power applications, which includes wireless power transfer, induction heating and magnetic hyperthermia. The structure uses multiple foil layers cut into C-shapes with opposite orientations in successive layers. These C-shapes form inductive loops with integrated capacitance and currents in different layers are induced by inductive coupling. This structure has also been used to create high-Q coils for wireless power transfer and it resulted in high-efficiency energy transfer over a large range [17].

In this paper, we use similar capacitive ballasting strategy to achieve high-Q resonators with a multi-layer foil winding structure. The parallel resonator resonates at 12.99 MHz without magnetic cores and at 8.5 MHz with magnetic cores; the resonant frequencies for the series resonator are 12 MHz and 7.7 MHz respectively. Characterization of the resonator impedance shows that the prototype multi-layer parallel and series resonators with magnetic cores have quality factors of 835 and 838 respectively, about 1.5 times better than

resonators with similar inductance and capacitance using a single-layer winding. The resonator structure and the loss model for both the multi-layer and the single-layer resonators are presented, followed by experimental verification.

II. Resonator Structures

A. Single-Layer Resonator

A simple resonant structure for the MHz frequency range includes an inductor with a single-layer foil winding connected to a capacitor. The foil should be at least two skin depth thick so that high-frequency current can flow along both sides of the conductor surface. Assuming that the capacitor connected to the winding has a high quality factor, the efficiency of the resonator is limited by twice the skin depth at the operating frequency.

B. Multi-Layer Resonator

This skin-effect limitation can be overcome by using a multi-layer winding design with equal current sharing among layers each of which are much thinner than a skin depth [15]. Fig. 1 shows how a multi-layer winding strategy, such as capacitive ballasting [15], can be incorporated to the foil winding of an inductor. In Fig. 1 (a), multi-layer conductors replace the two horizontal segments of an inductor with a single-layer winding. It provides a series resonance with a very low winding loss if the vertical dimensions (h and b) are small compared to the horizontal dimension l. The dielectric separating the conductor layers provides an integrated capacitance, thereby eliminating the need for connecting this inductor to additional capacitors, which further reduces the connection loss. This integrated capacitance is similar to the integrated LC and LCT (inductor, capacitor, transformer) devices discussed in [18]–[21]. However, the integrated capacitance in our resonator is implemented by a multi-layer winding with equal current sharing, thereby improving the winding efficiency in addition to a parts count saving due to integration.

For structures with similar horizontal and vertical dimensions, the multi-layer winding concept needs to be extended to the vertical segments. If the combined thickness of the conductor layers is small (i.e. $b \approx h$), a low-loss series resonance can be achieved with the structure in Fig. 1 (b). Winding losses can be further reduced if a multi-layer winding is used for all four segments as shown in Fig. 1 (c), but it gives a parallel resonance, rather than a series resonance.

Both the parallel resonator (Fig. 1 (c)) and the series resonator (Fig. 1 (b)) were modeled and built for testing the benefit of using the multi-layer winding structure. The construction of the parallel resonator is easier since it involves only layering the conductor and the dielectric strips whereas the series resonator also requires cutting and soldering these strips together. The two resonators have similar losses if $b \approx h$ and if the strips of the series resonator can be soldered together without introducing significant losses.

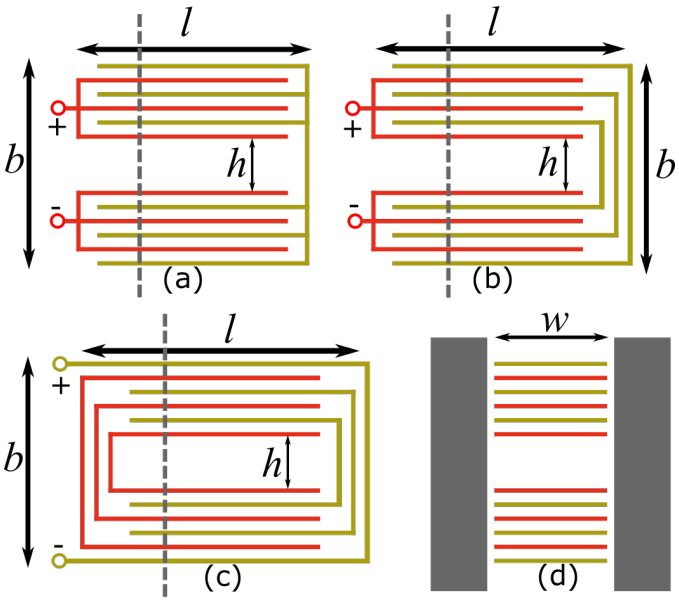

Fig. 1. Various resonator structures with multi-layer windings. (a) and (b) are series resonators and (c) a parallel resonator. The structures extend a width w perpendicular to the page. (d) is the cross-section of the resonators (a)–(c) along the dashed lines, with magnetic cores (grey) to straighten the field lines.

C. High-Loss Substrate Integration

A high-Q multi-layer resonator for MHz frequencies, as mentioned above, requires conductors which are much thinner than a skin-depth, and so are hard to handle. It also requires dielectric layers with a low dissipation factor, such as PTFE. Although laminates of a thin layer of copper on a thicker dielectric substrate are easier to handle, laminates using a low-loss dielectric are very expensive. Thus, a resonator with similarly low loss, but one which can be built using free-standing PTFE sheets and the industry-standard polyimide laminate coated with thin layers of copper, is desirable.

This can be achieved by modifying the parallel resonator as shown in Fig. 2 (a), in which each copper layer in Fig. 1 (c) is replaced with a laminate consisting of a layer of polyimide substrate coated on both sides by thin copper layers. These laminates and free-standing PTFE strips are stacked together around a center mandrel, with successive pairs wrapped around opposite ends of the mandrel such that the openings of the successive pairs face opposite directions.

This modified resonator can be represented by the equivalent circuit model as shown in Fig. 2 (b). The PTFE dielectric in the region of overlap between two successive laminate strips forms the integrated capacitance, represented by C_{LL} for each layer; a low-loss dielectric, i.e. PTFE, is used because a strong electric field is generated in this region to transfer current between adjacent copper layers. On the other hand, the two copper layers of each laminated strip are grouped together and so the polyimide substrate does not experience a strong electric field; therefore, it does not significantly contribute to the loss. In the equivalent circuit model in Fig. 2 (b), this is represented by an equivalent capacitor C_{HL} connected to points of the same potential on successive conductor layers, thus contributing neither capacitance nor loss.

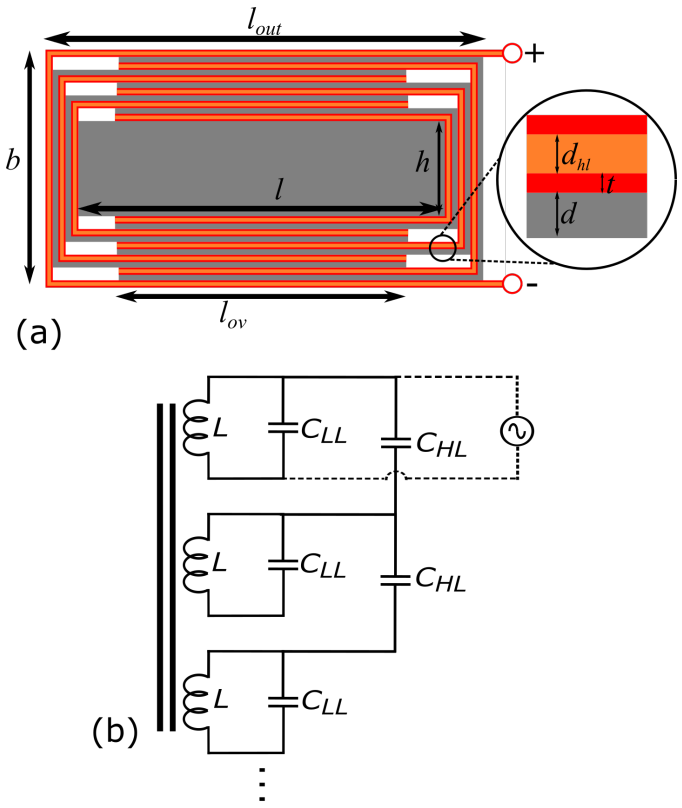

Fig. 2. (a) A sample cross-section of the parallel resonator with integrated capacitance using 6 copper strips (5 sections). Each copper strip is made up of high-loss dielectric such as polyimide (brown) coated on both side by copper (red). Low-loss dielectric such as PTFE (grey) separates the copper strips. The resonator extends a width w perpendicular to the page. (b) The circuit model, showing three sections, representing the modified resonator. The capacitor representing the high loss dielectric C_{HL} connects two points of the same potential on different layers and so does not experience a strong electric field.

This modified parallel resonator in Fig. 2 (a) can be built much more easily than the parallel resonator in Fig. 1 (c). The copper-polyimide-copper laminates are easier to handle than thin layers of free-standing copper. Moreover, free-standing PTFE sheets are much cheaper than PTFE laminates coated with thin layers of copper. Although the high-loss polyimide substrate is used, the resonator performance is not compromised because the substrate layers do not experience any strong electric fields.

III. Loss Model

The total loss of the resonator comprises the winding loss, including proximity effect and lateral current crowding, the dielectric loss for the multi-layer structure or the loss in the capacitors for the single-layer structure, and the core loss. These losses are represented by effective series resistance (ESR), as derived below.

A. Winding loss

A parallel self-resonant structure for wireless power transfer, similar to Fig. 1 (c) but with different shape and curvature, is described in [16]. That resonator is made of multiple conductor layers cut into C-shapes, with openings of the C-shape facing opposite directions in the successive layers. Such a resonant coil for wireless power transfer, built using high-loss substrate as described in Section II-C, is demonstrated in [17] to have a high quality factor. The winding resistance of such a structure is derived in [16] and is given by

$$R_w = \frac{R_{LF,loop}}{M} k_1 F_r, \tag{1}$$

$$F_r = 1 + \frac{M^2}{9}\left(\frac{t}{\delta}\right)^4 \frac{k_2}{k_1}, \tag{2}$$

where t is the thickness of the conductor layers, $R_{LF,loop}$ is the resistance of a conductor layer with the same thickness t that completes a full loop around the resonator, F_r the ac resistance factor, M the number of sections, each consisting of two consecutive conductor layers in opposite orientations separated by a low-loss dielectric, δ the skin depth, and k_1 and k_2 constants which are functions of the ratio of the overlapping length between consecutive layers to the total length around the resonator.

This ESR model in (1) and (2) can be used for the modified parallel resonator in Fig. 2, with the following adaptations. The number of sections M is one fewer than the number of conductor-polyimide-conductor strips. $R_{LF,loop}$ can be written as

$$R_{LF,loop} = \frac{\rho\ 2(l_{ave} + b_{ave})}{wt}, \tag{3}$$

$$l_{ave} = \frac{l_{out} + l}{2}, \qquad b_{ave} = \frac{h + b}{2}.$$

where ρ is the resistivity of the conductors, l_{ave} and b_{ave} average dimensions of the resonator as layers are stacked and w the width of the resonator perpendicular to the page; l, l_{out}, h and b are as shown in Fig. 2. The average dimensions of the resonator l_{ave} and b_{ave} are used in calculating $R_{LF,loop}$ because the loop length increases as the layers are stacked. The constants k_1 and k_2 are given by

$$k_1 = 1 - \frac{r_l}{3}, \tag{4}$$

$$k_2 = 1 + r_l, \tag{5}$$

$$r_l = \frac{l_{ov}}{l_{ave} + b_{ave}}, \tag{6}$$

where l_{ov} is average of the overlapping lengths and r_l the overlapping length as a fraction of the average length around the resonator.

The winding loss in (1) and (3) is based on assuming that the magnetic field lines are parallel to the conductor layers. However, in practice, fringing field lines cause current crowding at the conductor edges, inducing additional eddy currents and hence higher loss. This can be partially solved by adding low-loss magnetic cores at the two ends of the resonators, as shown in Fig. 1 (d), to straighten the field line. Moreover, this model for proximity effect losses also assumes that magnetic cores used together with the windings have infinite permeability; using cores with finite permeability

will weaken the magnetic flux density, resulting in a lower proximity effect loss than is predicted by the ac resistance factor F_r in (2). These field-weakening and current-crowding effects can be incorporated into (2) as

$$F_r' = 1 + \frac{M^2}{9}\left(\frac{t}{\delta}\right)^4 \frac{k_2}{k_1} F_{fw} + F_{cc}, \tag{7}$$

where F_{fw} and F_{cc} represent correction factors for field weakening and current crowding respectively.

These field weakening and current crowding effects can be quantified using 2D finite element method (FEM) simulations with and without magnetic cores. The FEM simulations are performed at dc and at the resonant frequency to obtain the ac and dc resistances R_{ac} and R_{dc}. However, the 2D simulations cannot exactly capture the effect of current transfer from one copper layer to the other copper layer in the same section. In addition, the simulations with M sections will have the proximity effect of a winding with $2M$ layers. These modifications give the ac resistance of the simulated resonant structure:

$$R_{ac} = R_{dc}\left(1 + \frac{(2M)^2}{9}\left(\frac{t}{\delta}\right)^4 F_{fw} + F_{cc}\right). \tag{8}$$

The middle term in the equation represent the resistance due to the proximity effect and can also be calculated using the average of the square of the peak magnetic flux density in the winding region $\langle \hat{B}^2 \rangle$ [16], [17] extracted from the simulation result. Equating the proximity effect loss calculated in this way to the middle term in (8) gives the field-weakening factor F_{fw}, which in turns can be substituted into (8) to get F_{cc}.

Substituting these factors F_{fw} and F_{cc} into (7), the winding resistance can be rewritten as

$$R_w = \frac{R_{LF,loop}}{M} k_1 F_r'. \tag{9}$$

B. Dielectric and Magnetic Core Losses

Although a multi-layer resonator potentially has a lower winding loss than a single layer inductor connected to a high-Q capacitor, the former requires dielectric layers and magnetic cores which introduce additional losses. The ESR for the dielectric loss R_{DF} can be written as

$$R_{DF} = \frac{D_f}{\omega C}, \tag{10}$$

where D_f is the dielectric dissipation factor of the low-loss dielectric material, ω the angular frequency and C the total integrated capacitance. The high-loss dielectric material does not experience any strong electric fields and so does not contribute to the dielectric loss. The ESR for the core loss R_c depends on the reluctances in air $\mathcal{R}_a$ and the core $\mathcal{R}_c$:

$$R_c = \Re\left(\frac{j\omega}{\mathcal{R}_a + \mathcal{R}_c}\right). \tag{11}$$

Because the reluctances depend on the flux lengths and areas, which in turns depend on the magnetic field configuration, they cannot be easily calculated directly. We approximate them as follows. The inductance of the resonator with the magnetic core L_C and that without the magnetic core L_{NC} can be written as

$$L_C = \frac{1}{\mathcal{R}_a + \Re(\mathcal{R}_c)}, \tag{12}$$

$$L_{NC} = \frac{1}{\mathcal{R}_a + \mathcal{R}_{a'}}, \tag{13}$$

where $\mathcal{R}_{a'}$ is the reluctance in the air in the region otherwise occupied by the magnetic cores and is related to $\mathcal{R}_c$ by

$$\mathcal{R}_c = \frac{\mathcal{R}_{a'}}{\mu_i - j\mu_{ii}}, \qquad \Re(\mathcal{R}_c) \approx \frac{\mathcal{R}_{a'}}{\mu_i}, \tag{14}$$

where $\mu_i - j\mu_{ii}$ is the complex relative permeability of the cores. From (12)–(14), we get

$$\mathcal{R}_{a'} \approx \left(\frac{1}{L_{NC}} - \frac{1}{L_C}\right)\frac{\mu_i}{\mu_i - 1}, \tag{15}$$

$$\mathcal{R}_a = \frac{1}{L_{NC}} - \mathcal{R}_{a'}. \tag{16}$$

The ESR for the core loss R_c can be calculated by substituting (14)–(16) into (11).

C. Losses in the Single-Layer Resonator

The benefit of using the multi-layer structure can be quantified by comparing it with a single-layer resonator of similar inductance and capacitance values. The total loss of the resonator includes the winding loss and ESR of the capacitors and the cores. The winding resistance of the single-layer resonator is given by $R_{LF,loop}$ in (3), where t is the thickness of a conductor much thicker than a skin depth, multiplied by the FEM ac resistance factor F_{FEM}, defined as the ratio of ac and dc resistances R_{ac}/R_{dc} from finite element simulations. The dielectric loss in the case of the single-layer resonator is represented by the effective series resistance of the capacitors. The core loss is approximated using the same method described in Section III-B.

IV. Experimental Verification

A. Multi-Layer Resonator

A prototype of the parallel resonator shown in Fig. 2 was built with 50 strips of copper (49 sections), each made of 25.4 μm polyimide coated with 5 μm copper on both sides, cut into 13 cm × 1 cm pieces. The cutting process could introduce electrical shorts between the two sides of the same copper strip, and so the edges of the copper strips were etched with ammonium peroxydisulfate solution (20 wt%) to remove these electrical shorts. PTFE strips of 50.8 μm thickness with slightly larger dimensions separated the copper strips. The copper and PTFE strips were wrapped around a 3.81 cm × 3.81 cm PTFE block. The layers were held together by a clamping mechanism made from polypropylene. Magnetic cores made of Fair-Rite 67 material, which maintains a low loss up to around 10 MHz, were used to straighten the field lines. These dimensions and the material properties of PTFE and Fair-Rite 67 material are summarized in Table I. After

TABLE I
KEY PARAMETERS

Number of copper strips		50
Number of sections	M	49
Copper strip length	l_{Cu}	13 cm
Copper strip width	w	1 cm
Copper layer thickness	t	5 µm
High-loss dielectric (polyimide) thickness	d_{hl}	25.4 µm (1 mil)
Low-loss dielectric (PTFE) thickness	d	50.8 µm (2 mil)
PTFE block length	l	3.81 cm (1.5")
PTFE block thickness	h	3.81 cm (1.5")
PTFE block width		1.27 cm (0.5")
PTFE dielectric constant	ϵ_r	2.1
PTFE dissipation factor	D_f	0.0002
67 material relative permeability (real)[a]	μ_i	48
67 material relative permeability (imag)[a]	μ_{ii}	0.09 (8 MHz)
	μ_{ii}	0.14 (12 MHz)
	μ_{ii}	0.16 (13 MHz)
Resonator total length	l_{out}	$\approx$ 4.6 cm
Resonator total thickness	b	$\approx$ 4.6 cm
Adjacent-layer average overlap length	l_{ov}	$\approx$ 5 cm
Resonator average length	l_{ave}	4.2 cm
Resonator average thickness	b_{ave}	4.2 cm
Overlap-to-total length ratio (See (6))	r_l	0.595
A function of r_l (See (4))	k_1	0.802
A function of r_l (See (5))	k_2	1.595

[a] The values of relative permeability μ_i and μ_{ii} are measured using a thick wire loop and a closed pot core; the datasheet provides slightly different values.

impedance characterization, this multi-layer parallel resonator was transformed into a series resonator by simply cutting up one side of the resonator and soldering the layers of each end together. Fig. 3 (a) and (b) show the multi-layer series resonator, respectively without and with the magnetic cores of Fair-Rite 67 material.

To determine the losses of the multi-layer resonators, both without and with the magnetic cores of the 67 material, the impedances of the resonators were measured with an Agilent 4294A impedance analyzer. Fig. 4 shows the impedance characteristics of the parallel resonator and Fig. 5 that of the series resonator. In addition to the fundamental resonance, the multi-layer resonators have resonances at higher harmonics, indicating the presence of integrated capacitance. The resonators with magnetic cores have lower resonant frequencies and narrower resonance peaks than those without magnetic cores, indicating that adding the magnetic cores increases the quality factor and reduces the winding loss.

The resonant frequency, and the width and the peak of the fundamental resonance of the resonators were used to calculate the quality factor, the inductance and the capacitance, giving the results shown in Table II. The multi-layer parallel resonator without the cores has a quality factor Q of 185 at 12.99 MHz; when the cores are added, Q increases by a factor of 4.5, to 835, at 8.51 MHz. This large increase in the quality

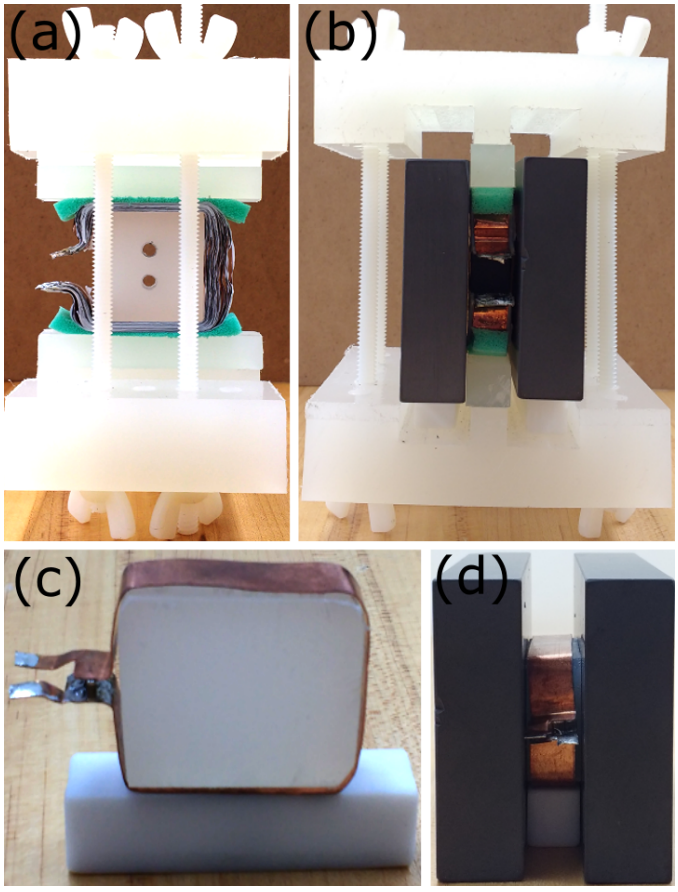

Fig. 3. (a) The prototype multi-layer series resonator. (b) The series resonator with magnetic cores of Fair-Rite 67 material to straighten field lines. (c) The single-layer parallel resonator. (d) The parallel resonator with magnetic cores.

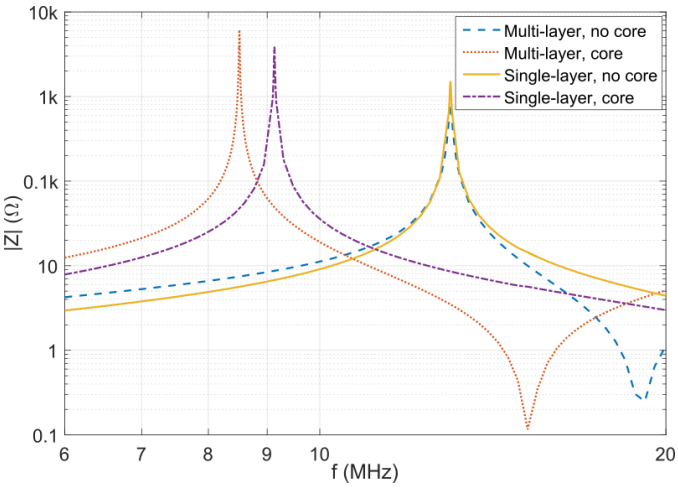

Fig. 4. Impedance vs. frequency for multi- and single-layer parallel resonators with and without magnetic cores. In addition to the fundamental parallel resonance, the multi-layer resonator has series and parallel resonances of higher harmonics.

factor shows that lateral current crowding is a significant problem in multi-layer resonators; magnetic cores alleviate this problem by straightening the field lines. The multi-layer series resonator has a similar quality factor, indicating that

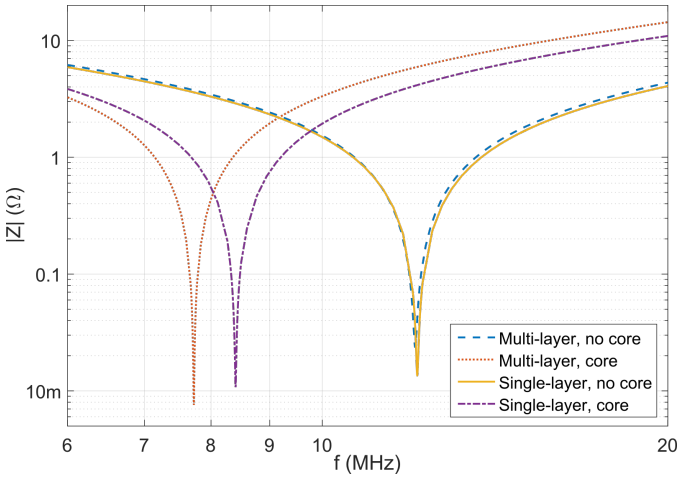

Fig. 5. Impedance vs. frequency for multi- and single-layer series resonators with and without magnetic cores.

soldering the conductor layers together does not contribute significant additional losses. The difference in the resonant frequency between the parallel and series resonator is due to the difference in capacitance, resulting from a difference in the clamping force.

In order to confirm that the loss model is correct and that adding magnetic cores reduces the winding loss, the losses due to the winding, the dielectric and the core were calculated as described in Section III, and the results are shown in Table II. The predicted quality factor agrees closely with the measured quality factor, confirming the loss model. The winding contributes the largest loss, from 72% to 96% of the total loss, of the multi-layer resonators. Adding the magnetic cores introduces core loss and increases the dielectric loss because the resonant frequency is lower. However, the decrease in the winding loss due to straighter magnetic field lines far outweighs the increase in the dielectric and the core losses. It should be noted that the straight field lines are not the only reason for the lower winding loss; the lower resonant frequency increases the skin depth, therby reducing the skin and proximity effects to some extent.

B. Single-Layer Resonator

Single-layer resonators of similar inductance and capacitance values weare also constructed to quantify the benefit of using the multi-layer structure. These single-layer resonators were made of 254 μm-thick copper ($>$ twice the skin depth around 10 MHz), cut into a 1 cm wide strip. The length of the strip was chosen to be 13 cm, which gave the same inductance as the multi-layer resonator. High-Q NP0 ceramic capacitors (ATC 800B series) were connected with the single-layer foil loop. Fig. 3 (c) and (d) shows the single-layer parallel resonators without and with the magnetic cores. The measured impedances of the single-layer parallel and series resonators are shown in Fig. 4 and Fig. 5 respectively. The losses were also calculated using the loss model in Section III and the results are shown in Table II. The measurement and the theory agrees closely, which further confirms the loss model.

The measured and predicted quality factors and losses of the single-layer resonators follow the same trends as those of the multi-layer resonators: the quality factor is higher when magnetic cores are added and the winding loss is the major portion of the total loss. However, the capacitor contributes larger loss in the single-layer resonator than the dielectric does in the multi-layer resonator, which may be attributed to the conduction losses and the proximity effect in the electrode plates of the lumped capacitors. Moreover, the single-layer resonators without magnetic cores have higher quality factors and lower winding resistances than do the multi-layer resonators, indicating that lateral current crowding is less significant for single-layer windings. This is supported by the fact the adding magnetic cores reduces the winding loss only by 36% in single-layer resonators, compared to 70% in multi-layer resonators.

V. Discussion

Both the measurement and the loss model show that a multi-layer resonator has a higher quality factor than a single-layer resonator, but only when magnetic cores are used to straighten the field lines to be parallel to the conductor layers. Thus, if magnetic cores are not available or cannot be used due to other limitations, a single-layer winding is better than a multi-layer winding not only for lower loss, but also for ease of construction. If magnetic cores can be used, however, a multi-layer winding provides at least 50% improvement. One exception is coil structures, such as toroids, with field lines inherently parallel to conductors; multi-layer windings will have lower loss than single-layer windings for these structures regardless of the magnetic cores. It should be noted that the improvement can be much larger than 50% if the designs of the resonators are further optimized. For example, using a circular cross-section for the resonators, rather than the square cross-section described in this paper, can improve the quality factors of both multi-layer and single-layer resonators by a factor of $\sqrt{4/\pi}$. Other parameters for design optimizations include the number of conductor layers, the conductor thickness, the distance between the conductor edges and the core, and the core shape.

The number of copper strips or sections M and the copper layer thickness t of the multi-layer resonators in this paper were not optimized to reduce the winding resistance, but chosen based on commercial availability. The proximity effect, with field lines parallel to the conductor layers, can be modeled using (1) and (2) and so M and t can be optimized to reduce this proximity effect. However, a multi-layer resonator optimized for reducing the proximity effect may not have the optimal design for overall winding loss; as evidenced in the experiment and the loss model, field weakening and lateral current crowding are significant factors in the winding resistance. Even though FEM simulations are useful for modeling these effects for particular designs, they cannot be used for design optimization; a closed-form model for these field weakening and lateral current crowding effects are required to minimize the winding resistance.

TABLE II
CHARACTERIZATION OF THE RESONATORS

	Measured				Model			
	f(MHz)	Q	L (nH)	C (nF)	R_w(mΩ)	$R_{DF}{}^a$	Q	
Multi-layer								
Parallel, No core	12.99	**185**	54.56	2.75	18.48	0.89	-	**231**
Parallel, 67 core	8.51	**835**	137.60	2.54	5.44	1.47	0.46	**999**
Series, No core	12.05	**174**	54.24	3.22	17.93	0.82	-	**220**
Series, 67 core	7.73	**838**	131.07	3.24	5.53	1.27	0.30	**930**
Single-layer								
Parallel, No core	12.99	**326**	56.16	2.67	11.07	2.93	-	**327**
Parallel, 67 core	9.13	**583**	114.63	2.65	7.11	3.27	0.34	**613**
Series, No core	12.10	**290**	51.59	3.35	10.66	2.26	-	**303**
Series, 67 core	8.40	**519**	105.91	3.39	6.81	2.57	0.24	**581**

[a] R_{DF} for the single-layer resonator is the effective series resistance of parallel combinations of ATC 800B capacitors, measured with a precision impedance analyzer. The combined ESR calculated from the ATC datasheet is larger, around 7 mΩ.

The distance between the core and the conductor edges also affects the winding resistance by changing the field-weakening and the lateral current crowding factors, expressed by F_{fw} and F_{cc} in (7). Because of the limitations in building the resonator, the magnetic cores could not be placed infinitesimally close to the edges of the conductors. The gap between the conductor edges and the core in our prototype was measured to be around 2 mm. The winding losses for the resonators with the cores in Table II were calculated using this 2 mm gap in the FEM simulation. The simulation was repeated with a few different gap distances and the winding losses for the different gap distances are shown in Fig. 6. It can be seen that, for our prototype, the multi-layer structure has a lower winding loss than the single-layer structure if the gap between the core and the conductor edges is less than about 3 mm. The benefit for multi-layer structure is larger if the core gets closer to the conductor edges because the field lines become straighter.

This decrease in the winding loss with decreasing gap distance can also be considered as a redistribution of the loss from the winding to the magnetic cores. The winding loss is reduced as the core gets closer to the conductor edges, but the core loss is increased because of an increase in the ratio of the reluctance of the magnetic path in the core to that in the air. As shown in Table II, the winding loss is over 66% of the total loss whereas the contribution from the core loss is around 5%. This indicates that redistributing the loss from the winding to the core can potentially reduce the total loss. This redistribution can also be done by changing the core shape, extending the core along the middle of the resonator for instance, which increases the reluctance of the magnetic flux path inside the core. This can also be seen in [17], in which the multi-layer winding is placed inside a pot core, resulting in the winding loss and the core loss of the same order of magnitude.

The reduction of the winding loss is not the only benefit of using the multi-layer structure with the magnetic cores. The integrated capacitance means that the plate resistance in the lumped capacitors and the capacitor-inductor connection loss are eliminated. As shown in Table II, the dielectric loss in the multi-layer structures is around 1 mΩ and the capacitor ESR in the single-layer structures is around 3 mΩ, indicating that about 2 mΩ can be reduced by using the multi-layer structure, which provides integrated capacitance.

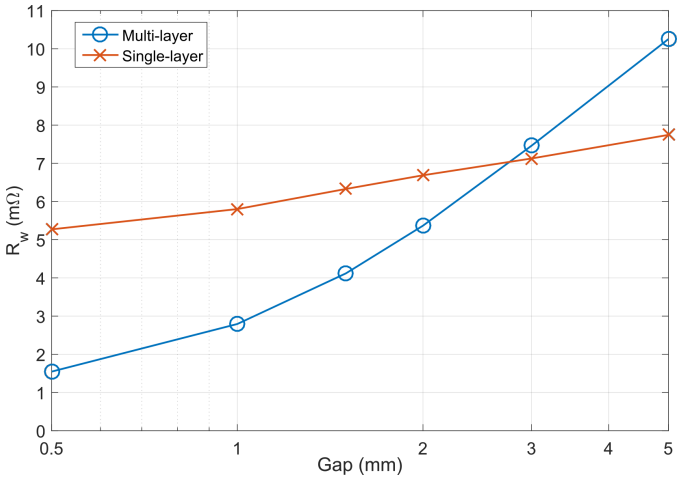

Fig. 6. Winding resistance as a function of the distance between the core and the edges of the conductor. The multi-layer resonator was simulated at 7.73 MHz and the single-layer resonator at 8.40 MHz, corresponding to the series resonators with magnetic cores. When the core is close to the conductors, the multi-layer resonator is less lossy because the field lines are straight. As the core moves farther away, the resistance of the multi-layer resonator increases rapidly.

It should be noted that the multi-layer resonator presented in this paper was designed for a high quality factor rather than a high energy density. A resonator optimized for a high energy density will have a large portion of the available space dedicated for capacitors since they have higher energy densities than inductors. Moreover, the choice of dielectric will also be based on the dielectric constant and the electric breakdown field in addition to the low dissipation factor used in this paper. Such a resonator will have a low quality factor because of a high capacitance required to achieve a high energy density. Optimization of resonators based on these criteria can be found in [22].

VI. Conclusion

Resonators with a multi-layer foil winding with high quality factors were presented. With magnetic cores to straighten the field lines, the parallel resonator has a quality factor of 835 at 8.51 MHz and the series resonator 838 at 7.7 MHz. These quality factors are about 1.5 times that of the next best alternative at MHz frequencies, an inductor with a single-layer foil winding in parallel with high-Q capacitors.

Losses in both the multi-layer and the single-layer resonators are also modeled, considering the winding loss, the dielectric loss or the capacitor ESR, and the core loss. The quality factors predicted by the loss model match closely with the measured quality factors. According to the model, the multi-layer resonators have a higher quality factor than the single-layer resonators due to lower winding and dielectric losses. The winding loss is lower because the multi-layer structures are not limited by the skin depth; however, the winding loss is reduced only when the magnetic cores are close enough to the conductor edges to provide straight field lines. The dielectric loss is lower because the integrated capacitance in the multi-layer structure eliminates the capacitor plate resistance and the need for capacitor-inductor connection.

The high quality factor means that frequency dependent skin and proximity effect losses in the MHz frequency range can be reduced by using a multi-layer foil winding with capacitive ballasting. In terms of power conversion, these high-Q multi-layer resonators can be used in place of LC resonant tanks in switching power converters. The lower conduction losses in these multi-layer resonators, in conjunction with the better performance of wide-bandgap devices compared to traditional MOSFETs, mean that entire resonant power converters can be more efficiently operated at MHz frequencies, allowing for smaller sized converters for the same power rating and allowable temperature rise.

References

[1] D. J. Perreault, J. Hu, J. M. Rivas, Y. Han, O. Leitermann, R. C. N. Pilawa-Podgurski, A. Sagneri, and C. R. Sullivan, "Opportunities and challenges in very high frequency power conversion," in *24th Annual IEEE Applied Power Electronics Conference and Exposition (APEC)*, 2009, pp. 1–14.

[2] M. F. S. John G. Kassakian, "High-frequency high-density converters for distributed power supply systems," *Proceedings of the IEEE*, vol. 76, no. 4, pp. 362–376, 1988.

[3] D. Maksimovic, "A MOS gate drive with resonant transitions," in *22nd Annual IEEE Power Electronics Specialists Conference (PESC)*, 1991, pp. 527–532.

[4] C. R. Sullivan, D. V. Harburg, J. Qiu, C. G. Levey, and D. Yao, "Integrating magnetics for on-chip power: A perspective," *IEEE Transactions on Power Electronics*, vol. 28, no. 9, pp. 4342–4353, 2013.

[5] C. R. Sullivan, D. Yao, G. Gamache, A. Latham, and J. Qiu, "(invited) passive component technologies for advanced power conversion enabled by wide-band-gap power devices," *ECS Transactions*, vol. 41, no. 8, pp. 315–330, 2011.

[6] R. C. N. Pilawa-Podgurski, A. Sagneri, J. M. Rivas, D. I. Anderson, and D. J. Perreault, "Very high frequency resonant boost converters," in *IEEE Power Electronics Specialists Conference*, 2007, pp. 2718–2724.

[7] N. Butzen and M. Steyaert, "12.2 a 94.6%-efficiency fullyintegrated switched-capacitor dc-dc converter in baseline 40nm CMOS using scalable parasitic charge redistribution," in *IEEE Internatoinal Solid-State Circuits Conference (ISSCC)*, 2016, pp. 220–221.

[8] J. Stauth, "Resonant switched capacitor power converters and architectures," in *Power Mangement Integrated Circuits*, M. M. Hella and P. Mercier, Eds. Boca Raton, FL: CRC Press, 2016, pp. 145–170.

[9] C. Schaef and J. T. Stauth, "A 3-phase resonant switched capacitor converter delivering 7.7 W at 85% efficiency using 1.1 nH PCB trace inductors," *IEEE Journal of Solid-State Circuits*, vol. 50, no. 12, pp. 2861–2869, 2015.

[10] K. Kesarwani, R. Sangwan, and J. T. Stauth, "Resonant-switched capacitor converters for chip-scale power delivery: design and implementation," *IEEE Transactions on Power Electronics*, vol. 30, no. 12, pp. 6966–6977, 2015.

[11] P. K. Sood and T. A. Lipo, "Power conversion distribution system using a high-frequency ac link," *IEEE Transactions on Industry Applications*, vol. 24, no. 2, pp. 288–300, 1988.

[12] D. M. Divan, "The resonant dc link converter–a new concept in static power conversion," *IEEE Transactions on Industrial Applications*, vol. 25, no. 2, pp. 317–325, 1989.

[13] A. Balakrishnan, H. A. Toliyat, and W. C. Alexander, "Soft switched ac link buck boost converter," in *Twenty-Third Annual IEEE Applied Power Electronics Conference and Exposition (APEC)*, 2008, pp. 1334–1339.

[14] M. Amirabadi, J. Baek, H. A. Toliyat, and W. C. Alexander, "Soft-switching ac-link three-phase ac–ac buck–boost converter," *IEEE Transactions on Industrial Electronics*, vol. 62, no. 1, pp. 3–14, 2015.

[15] C. R. Sullivan, "Layered foil as an alternative to litz wire: Multiple methods for equal current sharing among layers," in *IEEE 15th Workshop on Control and Modeling for Power Electronics (COMPEL)*, 2014, pp. 1–7.

[16] C. R. Sullivan and L. Beghou, "Design methodology for a high-Q self-resonant coil for medical and wireless-power applications," in *IEEE 14th Workshop on Control and Modeling for Power Electronics (COMPEL)*, 2013, pp. 1–8.

[17] A. L. F. Stein, P. A. Kyaw, and C. R. Sullivan, "High-Q self-resonant structure for wireless power transfer," in *Thirty-Second Annual IEEE Applied Power Electronics Conference and Exposition (APEC)*, 2017.

[18] M. Ehsani, O. H. Stielau, J. D. van Wyk, and I. J. Pitel, "Integrated reactive ccomponent in power electronic circuits," *IEEE Transactions on Power Electronics*, vol. 8, no. 2, pp. 208–215, 1993.

[19] J. A. Ferreira and J. D. van Wyk, "Electromagnetic energy propagation in power electronicconverterse: toward future electromagnetic integration," *Proceedings of the IEEE*, vol. 89, no. 6, pp. 876–889, 2001.

[20] E. Waffenschmidt and J. Ferreira, "Embedded passive integrated circuit for power converters," in *33rd Annual IEEE Power Electronics Specialists Conference (PESC)*, vol. 1, 2002, pp. 12–17.

[21] J. T. Strydom and J. D. van Wyk, "Volumetric limits of planar integrated resonant transformers: a 1 MHz case study," *IEEE Transactions on Power Electronics*, vol. 18, no. 1, pp. 236–247, 2003.

[22] P. A. Kyaw and C. R. Sullivan, "Fundamental examination of multiple potential passive component technologies for future power electronics," in *IEEE 16th Workshop on Control and Modeling for Power Electronics (COMPEL)*, 2015.